Raman study of $Bi_{2-x}Pb_xSr_2Ca_{n-1}Cu_nO_{4+2n+\delta}$ ($n=2,3$) superconductors

G. V. M. Williams and D. M. Pooke
New Zealand Institute for Industrial Research, P.O. Box 31310, Lower Hutt, New Zealand

D. J. Pringle and H. J. Trodahl
School of Chemical and Physical Sciences, Victoria University, P.O. Box 31310, Wellington, New Zealand

J. L. Tallon
New Zealand Institute for Industrial Research, P.O. Box 31310, Lower Hutt, New Zealand

J. Quilty
School of Chemical and Physical Sciences, Victoria University, P.O. Box 31310, Wellington, New Zealand

N. Malde
Department of Physics, Imperial College of Science, Technology, and Medicine, SW7 2BZ London, United Kingdom

J. L. Macmanus-Driscoll and A. Crossley
Department of Material Science, Imperial College of Science, Technology, and Medicine, SW7 2BP London, United Kingdom

L. F. Cohen
Department of Physics, Imperial College of Science, Technology, and Medicine, SW7 2BZ London, United Kingdom
(Received 9 September 1999)

We report a Raman study of the $n=2$ and $n=3$ $Bi_{2-x}Pb_xSr_2Ca_{n-1}Cu_nO_{4+2n+\delta}$ high-temperature superconducting cuprates. We find that the frequency of the $O(2)_{Sr}$ A_{1g} mode systematically decreases with additional oxygen in the weakly coupled BiO layers. We speculate that this could be due to an expansion of the Cu-O-Bi bond length caused by an oxygen-induced compression of the weakly coupled BiO layers. It is shown that approximately one half of the decrease in the frequency of the $O(2)_{Sr}$ A_{1g} mode in $Bi_2Sr_2Ca_{1-z}Y_zCu_2O_{8+\delta}$ reported by Kahihana *et al.* can be attributed to the effect of additional oxygen and hence charge transfer effects are negligible for this Raman mode. The effect of Pb on the frequency of the $O(2)_{Sr}$ A_{1g} mode, while being systematic, can not be explained. We attribute the small increase in hole concentration with increasing Pb concentration to a partial charge compensation by a reduction in oxygen content. We provide evidence that the 655 cm^{-1} peak can be attributed to apical oxygen sites at the boundaries of the supercell induced by the incommensurate modulation in the BiO layers.

INTRODUCTION

It is important to understand how the phonon modes in both $Bi_{2-x}Pb_xSr_2CaCu_2O_{8+\delta}$ [(Bi,Pb)-2212] and $Bi_{2-x}Pb_xSr_2Ca_2Cu_3O_{10+\delta}$ [(Bi,Pb)-2223] change with hole concentration. This is because phonon-mediated pairing was successful in accounting for superconductivity before the discovery of the high-temperature superconducting cuprates (HTSC). There now exist a number of theories of HTSC that assume a dominant or partial effect of phonon interactions where the strength of the phonon interactions possibly changes with hole concentration.[1,2]

Most of the Raman modes in Bi-2212 have been assigned but there is controversy surrounding the assignment of the 655 cm^{-1} peak. This peak has been assigned to a ''tetragonally forbidden (disorder-induced)'' [3] mode. Raman measurements on $Bi_2Sr_2Ca_{1-z}Y_zCu_2O_{8+\delta}$ have also found that the change in the frequency of the $O(2)_{Sr}$ A_{1g} mode is too great to be explained by internal pressure effects (i.e., an increase in the Cu-O-Bi bond length) and hence it was deduced that this mode is also affected by charge transfer effects.[3] An understanding of the effect of Pb on the Raman modes in (Bi,Pb)-2212 and (Bi,Pb)-2223 is also important. It was initially hoped that Pb^{2+} would substitute onto the Bi^{3+} site, yet there is no evidence of the expected large increase in hole concentration. It has been reported that a Pb-induced Raman mode near 540 cm^{-1} mode could be due to a Cu-O-Pb vibration.[4]

In this paper we report a systematic Raman study of polycrystalline (Bi,Pb)-2212 and (Bi,Pb)-2223. Raman spectroscopy has proved to be a useful characterization tool due to its ability to probe small regions and its nature as a probe of the local atomic configurations through shifts in the phonon frequencies.[5,6] We concentrate on polycrystalline samples, rather than single crystals, because it is not yet possible to make single crystals of the $n=3$ phase of suitable size and quality. We show below that the Raman $O(2)_{Sr}$ A_{1g} mode changes systematically with increasing oxygen concentration. There has been one study on Bi-2212 where the Raman spectra from three samples ''as prepared,'' ''annealed in O_2,'' and ''annealed in N_2'' are presented.[7] Unfortunately the T_c values were not reported and hence it is impossible to

 ©2000 The American Physical Society

determine the hole concentration for the three annealing conditions. Furthermore, the authors report a shift in the frequency of this mode by 9.5 cm^{-1}. We show in our systematic study that the shift in the frequency of this mode is no more than 3.5 cm^{-1}. We also show that the shift in frequency of this mode can be attributed to the additional oxygen and that any charge transfer effect is small. We discuss the assignment of the 655 cm^{-1} peak, the 540 cm^{-1} peak and the effects of Pb substitution.

EXPERIMENTAL DETAILS

Polycrystalline samples of $Bi_{2.1-x}Pb_xSr_{1.9}CaCu_2O_{8+\delta}$ were synthesized from a stoichiometric mix of Bi_2O_3, PbO, $Sr(NO_3)_2$, $Ca(NO_3)_2$, and CuO. The reaction was carried out at temperatures between 800 °C and 850 °C and oxygen partial pressures of between 1 and 21 %. The exact synthesis conditions depended on the desired Pb content with higher Pb contents requiring lower temperatures and oxygen partial pressures. X-ray diffraction (XRD) measurements indicated that all samples were single phase to within the detection limit of the spectrometer (i.e., <4% impurity level).

The $Bi_{2.1-x}Pb_xSr_{1.9}Ca_2Cu_3O_{10+\delta}$ polycrystalline samples were synthesized by successive reactions at 835 °C in 7.5% O_2 in N_2. The $x=0.6$ samples were reacted in 1% O_2 in N_2. The reaction times were typically 100 h. Note that both the $n=2$ and $n=3$HTSC were synthesised with 2.1 Bi and 1.9 Sr rather than the nominal 2.0 Bi and 2.0 Sr to account for the partial substitution of Bi onto the Sr site.[8] XRD measurements indicated that only the $x=0.6$ samples contained detectable quantities of the main lead-rich impurity phase $(Bi,Pb)_{3+y1}Sr_{2+y2}Ca_{2+y3}CuO_z$ which we refer to by the nominal indices 3221. Because the fraction of this impurity can change with subsequent oxygen annealing, sometimes appearing in samples of lower Pb content, we also characterized this phase using scanning electron microscopy and XRD. Using EDX analysis we determined a typical composition of $Bi_{0.33}Pb_{3.4}Sr_{2.6}Ca_{2.3}CuO_z$. This composition was then synthesized by reacting at 790 °C in flowing oxygen.

A sample of $Bi_{1.9}Pb_{0.2}Sr_{1.9}CaCu_2O_{8+\delta}$ was cut into halves and one half of the sample was annealed in ^{16}O while the other half was annealed in ^{18}O at 800 °C for 6 h and four repeat cycles. At the end of the final anneal the samples were cooled to 360 °C over 30 min and annealed at 360 °C for 24 h. Both samples were then co-annealed in a sealed evacuated quartz ampoule for 18 h at 400 °C in order to equalize their oxygen content and doping state without mixing isotopes on the CuO_2 planes.

$Bi_{2.1-x}Pb_xSr_{1.9}Ca_2CuO_{10-\delta}$ wire samples were supplied by the American Superconductor Corporation. The samples were embedded in resin and polished to expose the superconducting cores.

The oxygen content was altered by annealing the samples at different temperatures and oxygen partial pressures followed by quenching into liquid nitrogen. A sintered pellet was sectioned for each Pb concentration and each section was subject to different annealing conditions. Zero-field-cooled temperature-dependent susceptibility data was obtained using a vibrating sample magnetometer at an applied field of 0.3 mT. The room temperature thermopower, $S(300\,K)$, data was obtained using a technique described elsewhere [9] for all except the wire samples.

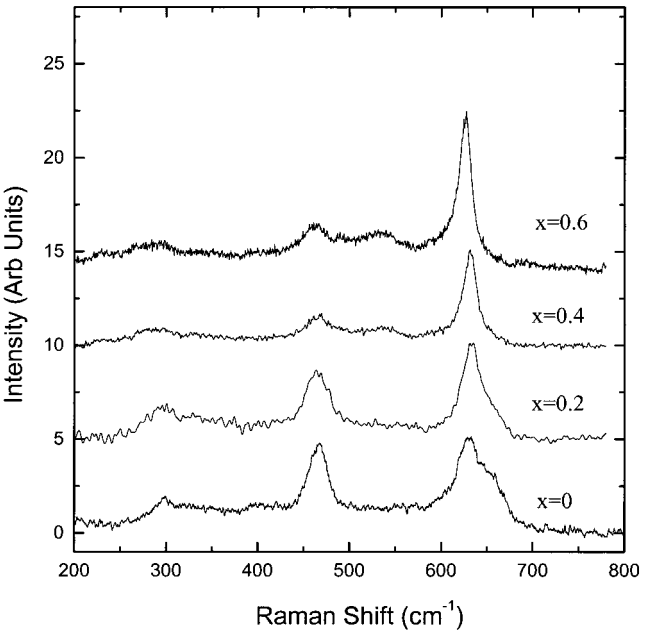

FIG. 1. Plot of the Raman spectra from $Bi_{2.1-x}Pb_xSr_{1.9}CaCu_2O_{8+\delta}$ polycrystalline samples for Pb contents indicated.

Raman measurements were made at room temperature using a backscattering geometry and the $\lambda=514.5$ nm line of an Ar ion laser. The power incident on the sample was <25 mW and the laser beam was focussed using a cylindrical lens to minimize possible thermal damage. The incident light was vertically polarized while the scattered light was observed without polarizers. However, as the vertical (V) polarized light is preferentially detected by the double monochrometer and CCD detector (a factor of ~3 over the horizontal polarization), then the primary detection is VV. The c-axis aligned superconducting wire samples were mounted with the long axis perpendicular to the incident polarization to observe scattering from the $O(2)_{Sr}$ A_{1g} Raman mode.

RESULTS AND ANALYSIS

We present in Fig. 1 typical spectra from polycrystalline samples of (Bi,Pb)-2212 with $x=0$, $x=0.2$, $x=0.4$, and $x=0.6$ all at similar hole concentrations. By comparison with previous studies we attribute the ~290, ~465, and ~630 cm^{-1} peaks to $O(1)_{Cu}$ B_{1g}, $O(3)_{Bi}$ A_{1g}, and $O(2)_{Sr}$ A_{1g} vibrations.[3,10] The O(1), O(2), and O(3) sites refer to the oxygen sites in the CuO_2, SrO, and BiO layers, respectively. The ~630 cm^{-1} peak observed in the $x=0$ and $x=0.2$ spectra also contains a high frequency shoulder which can be identified as the ~655 cm^{-1} peak observed in $x=0$ single crystals.[3]

There is some dispute as to the origin of 655 cm^{-1} peak. It has been assigned to a ''tetragonally forbidden (disorder-induced)'' mode,[3] excess oxygen in the BiO layers,[11] the $Bi_2Sr_2CuO_6$ phase or, more recently, to the effect of the incommensurate modulation in the BiO layers.[12] The assignment of this peak to excess oxygen in the BiO layers is inconsistent with polarization-dependent studies which indi-

cate that both the 630 and 655 cm^{-1} peaks arise from apical oxygen (i.e., Cu-O-Bi) vibrations along the *c* axis.[3] Furthermore, the assignment of the 655 cm^{-1} peak to a ''tetragonally forbidden (disorder-induced)'' mode is inconsistent with the rapid disappearance of this peak with increasing Pb substitution as can be seen in Fig. 1. We note that the rapid disappearance of the 655 cm^{-1} peak with increasing Pb concentration is consistent with a Raman study on a $Bi_{1.85}Pb_{0.19}Sr_{1.90}Ca_{1.17}Cu_2O_{8+\delta}$ single crystal[4,13] and a recent grazing incidence infrared reflectivity study of a $Bi_{1.6}Pb_{0.4}Sr_2CaCu_2O_{8+\delta}$ single crystal.[12] The ''tetragonally forbidden (disorder-induced)'' explanation is unlikely because the othorhombicity is known to increase with increasing Pb content, yet the 655 cm^{-1} peak intensity, relative to that of the ~630 cm^{-1} peak, is decreasing at the same time.[13] Furthermore, the relative intensity of the 655 cm^{-1} peak is not significantly affected by the substitution of Y onto the Ca site or La onto the Sr site, which would seem to exclude disorder effects.[3,14] We detect no intergrowths of $Bi_2Sr_2CuO_6$ in our Pb-free samples, which is inconsistent with the 655 cm^{-1} peak arising from $Bi_2Sr_2CuO_6$ intergrowths. Also, Raman studies on $Bi_2Sr_2Ca_{1-z}Y_zCu_2O_{8+\delta}$ (Ref. 3) show that the frequency of both the ~630 and 655 cm^{-1} peaks decrease together and by similar amounts with increasing Y concentration. Therefore, the most satisfactory explanation is that the 655 cm^{-1} peak arises from apical oxygen sites at the boundaries of the supercell.[12] The supercell arises from the incommensurate modulation of the BiO layers in which the BiO layers alternate between rocksalt and pseudo-perovskite packing with a mean period of 4.76*a* where *a* is the *a*-axis length.[15] The assignment of this mode is consistent with a recent calculation of the relative integrated intensities of the ~630 and ~655 cm^{-1} infrared peaks based on every fifth apical oxygen site having a different oscillator strength.[12] The experimental integrated intensities of the ~630 and ~655 cm^{-1} relative to the ~630 cm^{-1} infrared and Raman peaks are 4.6 and 4.7, respectively, for $x=0$, being close to the predicted value of around 4.[12] The rapid disappearance of the ~655 cm^{-1} peak with increasing Pb concentration can be explained by an increase in the supercell length [1.45 times greater for $x=0.19$ (Ref. 13)].

Another peak at ~540 cm^{-1} is visible in the $Bi_{2.1-x}Pb_xSr_{1.9}CaCu_2O_{8+\delta}$ Raman spectra for high Pb concentrations. This peak is not seen in single crystals when $x=0$ but it is seen in one study when $x>0$.[4] It has been suggested that this peak could be due to an intrinsic mode, however, it is more likely that it is due to a Pb-rich impurity phase. We show in Fig. 2(a) that the Raman spectra from the main Pb-rich 3221 impurity phase also have a peak near 540 cm^{-1}. Similar Raman spectra have also been obtained from Raman measurements on the Pb-rich 3221 phases by Wu *et al.*[16] where the intensity and widths of the four main peaks change with relative Pb and Bi ratios. It is important to note that the Pb-rich 3221 impurity Raman cross section is much greater than that for $Bi_{2.1-x}Pb_xSr_{1.9}CaCu_2O_{8+\delta}$ and hence the relative intensity of the ~540 cm^{-1} peak in the $Bi_{2.1-x}Pb_xSr_{1.9}CaCu_2O_{8+\delta}$ Raman spectra plotted in Fig. 1 would indicate an impurity fraction of less than 2% which is less than the fraction that can be detected by XRD (~4%).

Further evidence that the ~540 cm^{-1} peak arises from a Pb-rich impurity phase can be seen in Figs. 2(b) and 2(c)

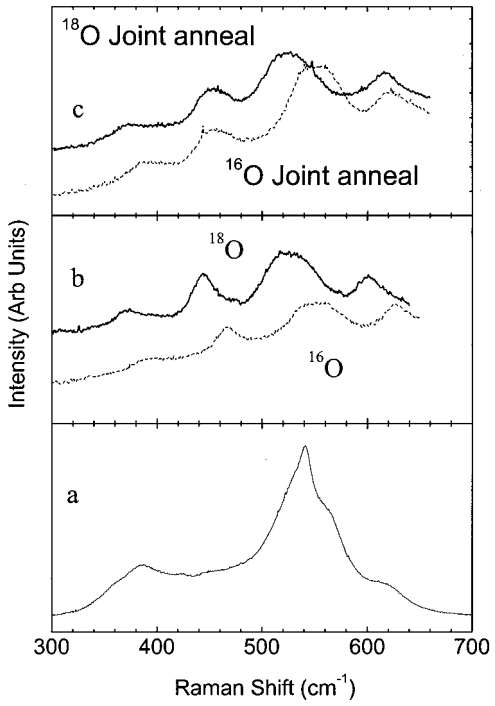

FIG. 2. Plot of Raman spectra from a $Bi_{0.33}Pb_{3.4}Sr_{2.6}Ca_{2.3}CuO_z$ polycrystalline samples (a), a $Bi_{1.9}Pb_{0.2}Sr_{1.9}CaCu_2O_{8+\delta}$ sample annealed in ^{16}O (dashed curve) or ^{18}O (solid curve) at 800 °C for 6 h and four cycles (b) and the same ^{16}O (dashed curve) and ^{18}O (solid curve) samples coannealed in a sealed evacuated ampoule at a lower temperature of 400 °C for 18 h (c).

where we plot Raman spectra from samples of $Bi_{1.9}Pb_{0.2}Sr_{1.9}CaCu_2O_{8+\delta}$ that have been ^{16}O or ^{18}O exchanged. In Fig. 2(b) we plot the Raman spectra from a $Bi_{1.9}Pb_{0.2}Sr_{1.9}CaCu_2O_{8+\delta}$ sample ^{16}O exchanged at 800 °C and a $Bi_{1.9}Pb_{0.2}Sr_{1.9}CaCu_2O_{8+\delta}$ sample ^{18}O exchanged at 800 °C for 6 h per exchange cycle and four repeat cycles. It is important to note that the samples were oxygen isotope exchanged at one atmosphere to promote the main Pb-rich impurity phase. It can be seen that in the ^{18}O exchanged sample the $O(3)_{Bi}$, ~540 cm^{-1} and $O(2)_{Sr}$ peaks all move to lower frequency consistent with 82% ^{18}O exchange. This is close to the estimate of 90% derived from the mass change. As noted earlier, these samples were then co-annealed in a sealed evacuated ampoule at a lower temperature of 400 °C for 18 h. It can be seen by comparing the Raman spectra in Figs. 2(b) and 2(c) that the effect of the coanneal is to shift both the $O(3)_{Bi}$ and $O(2)_{Sr}$ peaks consistent with 41% ^{18}O exchange on these two oxygen sites. However, the co-anneal has no effect on the position of the ~540 cm^{-1} peak. This indicates that this mode does not arise from the $O(2)_{Sr}$ or the $O(3)_{Bi}$ sites in $Bi_{1.9}Pb_{0.2}Sr_{1.9}CaCu_2O_{8+\delta}$. It is unlikely that the ~540 cm^{-1} peak arises from a $O(1)_{Cu}$ mode because this mode is seen at a much lower energy in $Bi_2Sr_2CaCu_2O_{8+\delta}$ (~290 cm^{-1} for B_{1g} and ~410 cm^{-1} for A_{1g}).[3] The simplest explanation is that the ~540 cm^{-1} peak arises from the impurity phase in which the oxygen diffusion kinetics are much slower than in the BiO and SrO layers of the superconducting phase.

We find that the apical $O(2)_{Sr}$ mode for (Bi,Pb)-2212 systematically decreases in frequency as samples are progres-

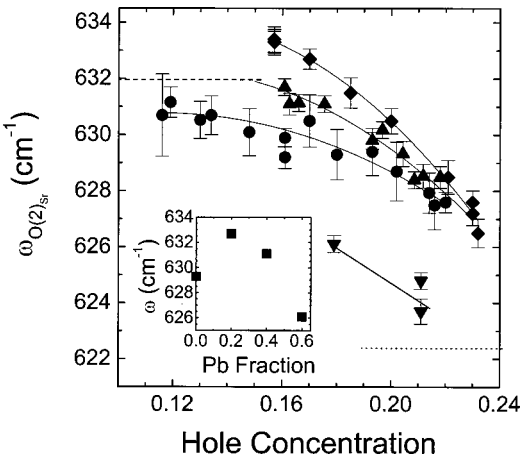

FIG. 3. Plot of the frequency of the $Bi_{2.1-x}Pb_xSr_{1.9}CaCu_2O_{8+\delta}$ $O(2)_{Sr}$ mode against hole concentration for Pb contents of $x=0$ (solid circles), $x=0.2$ (solid diamonds), $x=0.4$ (solid up triangles), and $x=0.6$ (solid down triangles). The curves are guides to the eye. The dashed curve is the maximum frequency reported by Chen *et al.* (Ref. 7) for the ''annealed in N_2'' sample and the dotted curve is the minimum frequency reported by Chen *et al.* for the ''annealed in O_2'' sample. Inset: Plot of the $Bi_{2.1-x}Pb_xSr_{1.9}CaCu_2O_{8+\delta}$ $O(2)_{Sr}$ mode against Pb content for a hole concentration near 0.175.

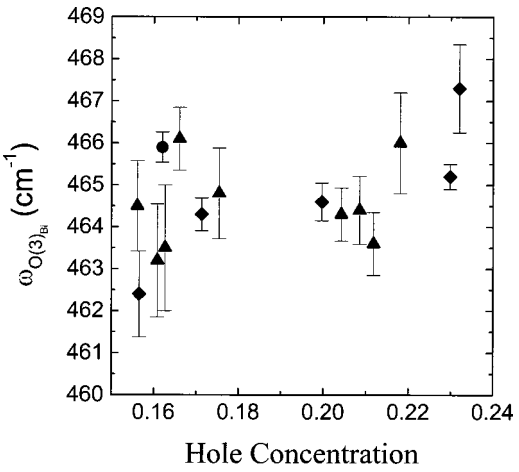

FIG. 4. Plot of the frequency of the $Bi_{2.1-x}Pb_xSr_{1.9}CaCu_2O_{8+\delta}$ $O(3)_{Bi}$ mode against hole concentration for $x=0$ (solid circle), $x=0.2$ (solid diamond), and $x=0.4$ (solid up triangles).

sively annealed in higher oxygen partial pressures or decreasing temperature. This can be seen in Fig. 3 where we plot the frequency of this mode against hole concentration for $x=0$ (filled circles), $x=0.2$ (filled diamonds), $x=0.4$ (filled up triangles), and $x=0.6$ (filled down triangles). The hole concentration was determined from the T_c values using the empirical relation $T_c \approx T_{c,\max}[1-82.6(p-0.16)^2]$ (Ref. 17) where $T_{c,\max}=95$ K and the thermopower correlation.[18] We plot the frequency against hole concentration because the hole concentration is easily estimated from T_c while δ is difficult to measure. Furthermore, changes in δ are small and there is little agreement in the literature on δ values even for similar T_c values.[19–21] As mentioned earlier, we are aware of only one other study where Raman spectra have been reported for Bi-2212 with different oxygen contents.[7] However, this study reported Raman spectra for only three annealing conditions described as ''as prepared.'' ''annealed in O_2,'' and ''annealed in N_2.'' The lack of T_c data means that it is impossible to accurately determine the hole concentrations. Furthermore the shift in the apical $O(2)_{Sr}$ mode for the most oxygenated sample reported by Chen *et al.* is anomalous.[7] This is apparent in Fig. 3 where we show the maximum (dashed line) and minimum (dotted) frequencies reported by Chen *et al.* The data of Chen *et al.* would seem to suggest a maximum hole concentration in excess of 0.24. This is inconsistent with previous studies. Furthermore, we estimate from the reported annealing conditions (500 °C in oxygen at 1 bar) that $p\sim0.19$. This estimate is consistent with $p\sim0.197$ estimated from another annealing study.[20] In our systematic study we find that the shift in the frequency of this mode is no more that 3.5 cm^{-1} compared with a shift of 9.5 cm^{-1} reported by Chen *et al.*

It can be seen in Fig. 4 that there is no evidence for a change in the frequency of the $O(3)_{Bi}$ mode with increasing oxygen content within experimental errors. Here we plot the frequency of the $O(3)_{Bi}$ mode against hole concentration for $x=0$ (solid circle), $x=0.2$ (solid diamond), and $x=0.4$ (solid up triangles). The limit on any possible correlation is less than 5 cm^{-1} over the doping range.

We show below that the systematic change in the apical oxygen mode frequency for progressively oxygen loaded (Bi,Pb)-2212 can be attributed to the additional oxygen in the BiO layers and that any charge transfer effect is small. It is important to first note that the correlation in Fig. 3 cannot be attributed to small changes in the unit cell volume. We find that for Bi-2212 the difference in unit cell volume between the most underdoped and most overdoped Bi-2212 sample is -0.3%. The effect of volume compression on the $O(2)_{Sr}$ mode can be estimated from the mode Grüneisen parameter, γ_i, defined as $\gamma_i=-d[\ln(\omega)]/d[\ln(v)]$, where ω_i is the phonon frequency and v is the volume. Using $\gamma_i=0.43$ (Ref. 22) we find that the decrease in the unit cell volume for $Bi_{2.1}Sr_{1.9}CaCu_2O_{8+\delta}$ should lead to the mode frequency increasing by 0.9 cm^{-1} rather than the experimentally-observed decrease of 3.5 cm^{-1}. We note that this decrease in frequency could be accounted for by a small increase in the Cu-O-Bi bond length of only $\sim1.3\%$.

To show that the changes in the apical $O(2)_{Sr}$ mode frequency with progressive oxygen loading can be accounted for by the increasing oxygen content rather than charge transfer effects, we compare our results with a study on $Bi_2Sr_2Ca_{1-z}Y_zCu_2O_{8+\delta}$ by Kakihana *et al.*[3] It was previously found that the frequency of the apical $O(2)_{Sr}$ mode decreases with increasing Y concentration.[3] This change was attributed to an internal pressure effect as well as a charge transfer effect. The internal pressure interpretation for $Bi_2Sr_2Ca_{1-z}Y_zCu_2O_{8+\delta}$ may be understood by the fact that Y^{3+} has a smaller ionic radius than Ca^{2+} [0.112 nm for Ca^{2+} compared with 0.1019 nm for Y^{3+} (Ref. 23)] leading to a contraction of the CuO_2 interlayer distance. However, the concomitant increase in oxygen content with increasing Y content[24] was not included in the analyses. This is important because the oxygen content increases by ~0.38 when z increases from 0 to 1. This can be compared with the estimated increase in oxygen content of ~0.12 (from a study by Shimoyama *et al.*[20]) as the hole concentration in Bi-2212 in-

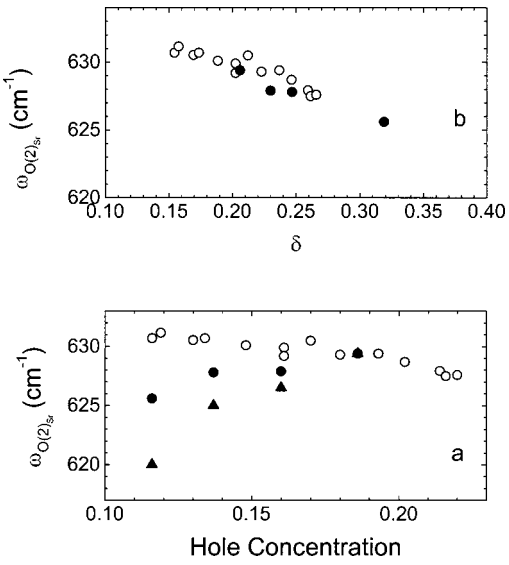

FIG. 5. Plot of the frequency of the $Bi_{2.1}Sr_{1.9}CaCu_2O_{8+\delta}$ (open circles) and $Bi_2Sr_2Ca_{1-z}Y_zCu_2O_{8+\delta}$ (solid up triangles) (Refs. 3, 19, 20, 24) $O(2)_{Sr}$ mode against hole concentration (a) or oxygen content δ (b). Also included is the frequency of the $Bi_2Sr_2Ca_{1-z}Y_zCu_2O_{8+\delta}$ $O(2)_{Sr}$ mode after removal of the effects due to the compression of the CuO_2 layers by different Ca^{2+} and Y^{3+} ionic radii (solid circles) as described in the text.

creases from the most underdoped to the most overdoped sample plotted in Fig. 3.

If charge transfer effects were significant then it would be expected that the frequency of the $O(2)_{Sr}$ mode should decrease with increasing hole concentration for both Bi-2212 and $Bi_2Sr_2Ca_{1-z}Y_zCu_2O_{8+\delta}$.[3] However, it is apparent in Fig. 5(a) that this is not the case. Here we plot the data from Fig. 3 (open circles) as well as the $Bi_2Sr_2Ca_{1-z}Y_zCu_2O_{8+\delta}$ data of Kakihana *et al.* (filled up triangles[3]). The additional anomalous frequency shift reported by Kakihana *et al.* and attributed to charge transfer effects can be seen by removing the effect of the contraction of the CuO_2 layers caused by the substitution of Y^{3+} for Ca^{2+}. We estimate the effect of the different ionic radii in the same manner as Kakihana *et al.* where the shift in the $O(2)_{Sr}$ mode was compared with the shift in the O_{Ba} A_g mode in $RBa_2Cu_3O_7$.[3] It was found that the frequency of the O_{Ba} A_{1g} mode decreases from 514 to 501 cm^{-1} when the rare earth atom is changed from Nd (ionic radii of 0.1109 nm) to Tm (ionic radii of 0.0994 nm).[25,26] Thus, we estimate that the contribution to the change in the frequency of the $O(2)_{Sr}$ mode in $Bi_2Sr_2Ca_{1-z}Y_zCu_2O_{8+\delta}$ by the different ionic radii of Y^{3+} for Ca^{2+} to be $\sim 14z$. However, even after the removal of the ionic nuclei size effect, it is apparent in Fig. 5(a) (solid circles) that the shift in the frequency of the $O(2)_{Sr}$ mode can not be consistently accounted for by charge transfer effects in Bi-2212 and $Bi_2Sr_2Ca_{1-z}Y_zCu_2O_{8+\delta}$.

It is clear in Fig. 5(b), after the removal of ionic radii effects in $Bi_2Sr_2Ca_{1-z}Y_zCu_2O_{8+\delta}$, that the frequency of the $O(2)_{Sr}$ mode in Bi-2212 and $Bi_2Sr_2Ca_{1-z}Y_zCu_2O_{8+\delta}$ is correlated with the oxygen content. The δ values for $Bi_2Sr_2CaCu_2O_{8+\delta}$ were estimated from a study by Shimoyama *et al.*[20] and the frequency of the $O(2)_{Sr}$ mode and δ values for $Bi_2Sr_2Ca_{1-z}Y_zCu_2O_{8+\delta}$ were estimated from studies by Kakihana *et al.*[3] and Groen *et al.*,[24] respectively. The additional oxygen could be affecting the $O(2)_{Sr}$ mode by causing a contraction of the weakly coupled BiO layers and an expansion of the Cu-O-Bi bond length. This interpretation is supported by evidence that additional oxygen is incorporated into the BiO layers in the boundary between the pseudo-perovskite and rocksalt phases.[15] While there is no systematic neutron diffraction data where the Cu-O-Bi bond length is reported as a function of oxygen content, we believe that there is no reason to state that the shift in frequency of the $O(2)_{Sr}$ mode is anomalous.[7]

It can be seen in Fig. 3 that Pb substitution has a significant effect on the frequency of the $O(2)_{Sr}$ Raman mode as well as the minimum hole concentration obtained for a constant low-pressure anneal. The effect of Pb substitution is more apparent in the inset to Fig. 3 where we plot the frequency of the $O(2)_{Sr}$ Raman mode against Pb content where the oxygen stoichiometry is controlled to give a constant hole concentration near 0.175. The origin of the initial increase and then decrease in the position of the $O(2)_{Sr}$ Raman mode with increasing Pb content is not obvious. It is difficult to model this effect as Pb introduces an additional incommensurate modulation[13] and little is known about the sites that Pb occupies. Pb could conceivably substitute onto the Bi, Sr, or Ca sites, although it is generally assumed to primarily substitute as Pb^{2+} on the Bi^{3+} site,[13] resulting in an increase in the hole concentration. There is evidence that Pb partially substitutes as Pb^{2+} on the Sr^{2+} site [$\sim$35% (Ref. 27)] without changing the hole concentration.[4,13] It has also been suggested that Pb substitutes predominately as Pb^{4+} on the Ca^{2+} site in $Bi_{2.1-x}Pb_xSr_{1.9}Ca_2Cu_3O_{10+\delta}$ (Ref. 28), however, this is not supported by a recent infrared study on a $Bi_{1.6}Pb_{0.4}Sr_2CaCu_2O_{8+\delta}$ single crystal.[12]

We speculate that the change in the frequency of the $O(2)_{Sr}$ mode with increasing Pb concentration could be due to a change in the relative distribution of the sites occupied by Pb as well as a decrease in oxygen content with increasing Pb concentration. That being said, there are several possible ways in which this could occur. One simple explanation is that for low Pb contents Pb substitutes onto the Bi sites with some Bi substituting onto the Sr site. As the Pb^{2+} ionic radius is greater than that for Bi^{3+},[23] this could lead to an increase in the BiO interlayer distance, a decrease in the Cu-O-Bi bond length and hence an increase in the $O(2)_{Sr}$ mode frequency. Note that no significant change is expected from any partial substitution of Pb^{2+} onto Sr^{2+} as Pb^{2+} and Sr^{2+} have similar ionic radii.[23] At high Pb contents, Pb could partially substitute as Pb^{4+} on the Ca^{2+} site. As the Pb^{4+} ionic radius is less than that of Ca^{2+},[23] then this could lead to a compression of the CuO_2 layers, an expansion of the Cu-O-Bi bond length and hence a decrease in the $O(2)_{Sr}$ mode frequency. Finally, one has to recognize that Pb^{4+} could preferentially substitute for Bi^{5+} in the perovskite domains in the BiO layers as might be suggested by the progressive disappearance of the 655 cm^{-1} mode.

A partitioning between sites and a decrease in oxygen content could also explain the small increase in hole concentration with increasing Pb content observed in Fig. 6 where

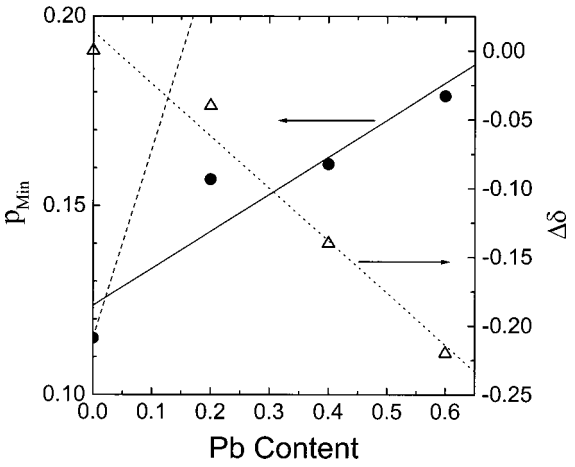

FIG. 6. Left vertical axis: Plot of the $Bi_{2.1-x}Pb_xSr_{1.9}CaCu_2O_{8+\delta}$ minimum hole concentration $p_{\min}$, against Pb content (filled circles). The solid line is a linear fit to the data and the dashed line is the expected line if each Pb contributed 1 hole to the CuO_2 planes. Right vertical axis: Plot of the $Bi_{2.1-x}Pb_xSr_{1.9}CaCu_2O_{8+\delta}$ change in oxygen content required if each Pb contributes 0.9 holes to the CuO_2 planes against Pb concentration (open up triangles). The dotted curve is a guide to the eye.

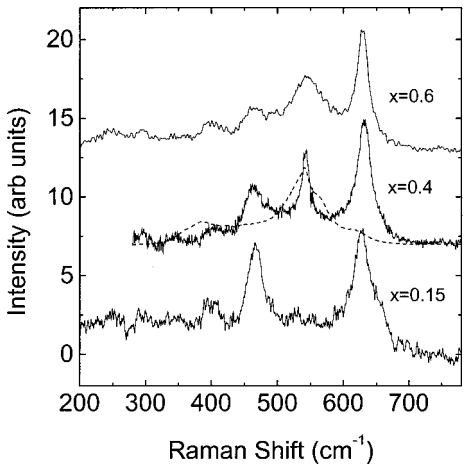

FIG. 7. Plot of the Raman spectra from $Bi_{2.1-x}Pb_xSr_{1.9}Ca_2Cu_3O_{10+\delta}$ polycrystalline samples with Pb contents of $x=0.15$, $x=0.4$, and $x=0.6$. The dashed curve is the Raman spectra from the main Pb-rich impurity phase $Bi_{0.33}Pb_{3.4}Sr_{2.6}Ca_{2.3}CuO_z$.

we plot the minimum hole concentration ($p_{\min}$) against Pb content (filled circles). The solid line represents 0.1 holes per Pb while the dashed line is the ideal of 1 hole per Pb expected for substitution only on the Bi site. It is possible that the additional holes introduced by Pb are partially compensated for by a decrease in oxygen content similar, but opposite to, the effect observed in $Bi_2Sr_2Ca_{1-z}Y_zCu_2O_{8+\delta}$ (Ref. 24) and $Bi_2Sr_{2-z}La_zCaCuO_{4+\delta}$,[29] where additional electrons are partially compensated for by an increase in oxygen content. In the case of $Bi_2Sr_2Ca_{1-z}Y_zCu_2O_{8+\delta}$ it is possible to show that, after accounting for the 1.8 holes per additional oxygen atom,[24] Y donates -0.9 holes per Y,[24] close to the maximum of -1 hole per Y. A similar analysis in the case of Pb substitution (assuming that Pb donates 0.9 holes per Pb atom and ignoring possible partial Pb substitution onto the Sr or Ca sites) would lead to changes in δ of up to -0.22 as can be seen in Fig. 6 (open triangles).

We now consider the Raman spectra for the triple CuO_2 layer $Bi_{2.1-x}Pb_xSr_{1.9}Ca_2Cu_3O_{10+\delta}$ polycrystalline samples plotted in Fig. 7. It is apparent from Figs. 1 and 7 that there are clear similarities between the spectra for (Bi,Pb)-2212 and (Bi,Pb)-2223. The $n=2$ and $n=3$ compounds both display the $O(3)_{Bi}$ A_{1g} and $O(2)_{Sr}$ A_{1g} phonon modes and the impurity mode near 540 cm^{-1}. The impurity mode is more intense and narrower for $x=0.4$ (and $x=0.34$) as can be seen in Fig. 7 where we plot the Raman spectra from the Pb-rich 3221 impurity phase (dashed curve). This may suggest that the main impurity phase for the $x=0.34$ and $x=0.4$ samples is possibly the (Sr,Ca,Pb) impurity phase or even Pb_3O_4.[15] The $x=0.15$ Raman spectra also displays the 655 cm^{-1} shoulder observed in the low Pb concentration (Bi,Pb)-2212 samples and, similarly, this shoulder is not evident for $x \geqslant 0.4$.

It can be seen in Fig. 8 that the frequency of the apical $O(2)_{Sr}$ mode in (Bi, Pb)-2223 also decreases with increasing oxygen content. Here we plot the data for $x=0.34$ and hole concentrations of $p=0.178$ (solid curve) and $p=0.139$ (dashed). It can be seen that the full width half maximum of the $O(2)_{Sr}$ mode increases with progressive oxygen loading. The resultant shift in the $O(2)_{Sr}$ mode from all our (Bi,Pb)-2223 samples is plotted in Fig. 9 for $x=0.15$ (open squares), $x=0.34$ (open circles), $x=0.4$ (open up triangles), and $x=0.6$ (open diamonds) against hole concentration where, for the determination of hole concentration, $T_{c,\max}$ is taken as 109 K. It is clear by comparison with Fig. 3 that $d\omega/dp$ is up to two times greater in the triple CuO_2 layer compound than in the double layer compound. It is not possible to estimate the δ values as no studies have been reported where δ has been reliably measured in the triple-layer compound. We have used the data in Fig. 9 to analyze a (Bi,Pb)-2223 tape with a nominal Pb content of $y=0.34$ and a resistive transi-

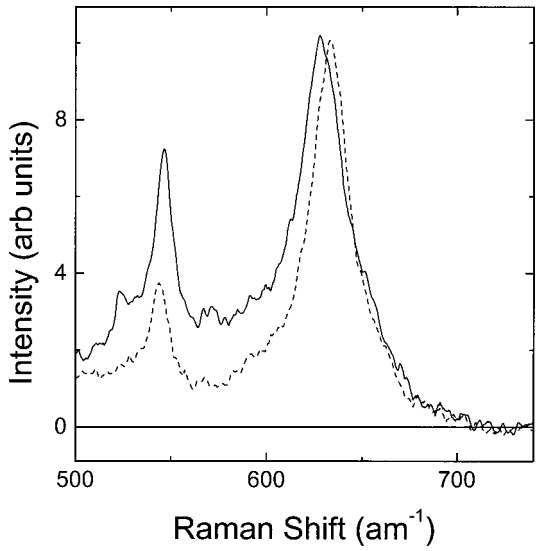

FIG. 8. Plot of the Raman spectra from a $Bi_{2.1-x}Pb_xSr_{1.9}Ca_2Cu_3O_{10+\delta}$ polycrystalline sample with $x=0.34$ and hole concentrations of $p=0.139$ (dashed curve) and $p=0.178$ (solid curve).

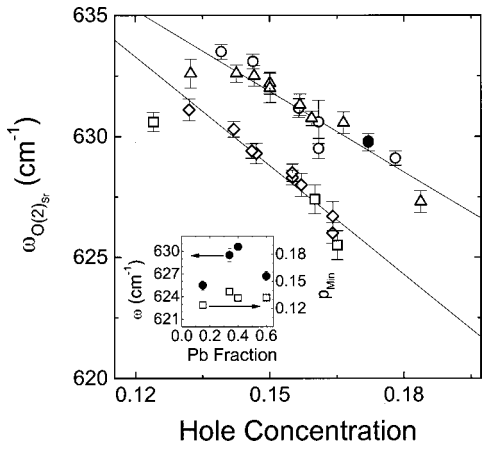

FIG. 9. Plot of the $O(2)_{Sr}$ mode frequency for $Bi_{2.1-x}Pb_xSr_{1.9}Ca_2Cu_3O_{10+\delta}$ against hole concentration for Pb contents of $x=0.15$ (open squares), $x=0.34$ (open circles), $x=0.4$ (open up triangles), and $x=0.6$ (open diamonds). The lines are linear best fits to the data. Also shown is the $O(2)_{Sr}$ mode frequency for a $Bi_{2.1-x}Pb_xSr_{1.9}Ca_2Cu_3O_{10+\delta}$ superconducting wire (solid circle). Inset: Left vertical axis: Plot of the $O(2)_{Sr}$ mode frequency for $Bi_{2.1-x}Pb_xSr_{1.9}Ca_2Cu_3O_{10+\delta}$ against Pb content for a hole concentration near 0.164 (filled circles). Right vertical axis: plot of the $Bi_{2-x}Pb_xSr_2Ca_2Cu_3O_{10+\delta}$ minimum hole concentration p_{min} against Pb content (open squares).

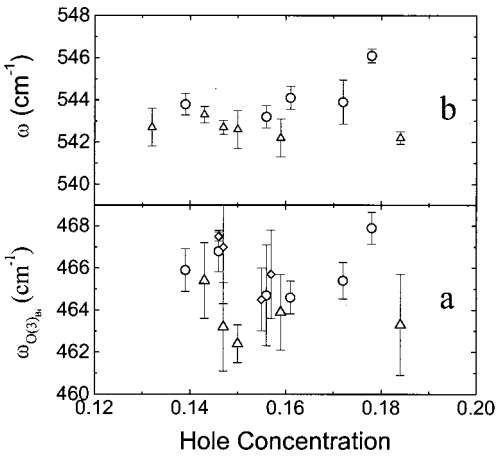

FIG. 10. Plot of the $O(2)_{Bi}$ mode frequency for $Bi_{2.1-x}Pb_xSr_{1.9}Ca_2Cu_3O_{10+\delta}$ against hole concentration for Pb contents of $x=0.34$ (open circles), $x=0.40$ (open up triangles), and $x=0.6$ (open diamonds) (a) and plot of the 3221 impurity peak frequency against hole concentration for Pb contents of $x=0.34$ (open circles) and $x=0.40$ (open up triangles).

tion at 107 K. The position of the $O(2)_{Sr}$ Raman mode is plotted on Fig. 9 by the solid circle which can be seen to fall on the $x=0.34$ and $x=0.4$ curves consistent with the nominal Pb content.

The triple-layer compounds also display similar changes in the $O(2)_{Sr}$ mode with increasing Pb concentration as can be seen in the inset to Fig. 9 where we plot the $O(2)_{Sr}$ mode frequency against Pb content (filled circles) for a hole concentration near 0.164. Unlike the double layer compounds, there is no significant change with Pb content in the minimum hole concentration obtained for the same low-pressure anneals. This is apparent in the inset to Fig. 9 where we also plot p_{min} against Pb content (open squares). The differences in p_{min} and the hole concentration range between the $n=2$ and $n=3$ compounds could be due to the different hole concentration distributions in the CuO_2 planes. NMR studies have shown that the holes are evenly distributed in the two CuO_2 planes for the $n=2$ compound while the middle CuO_2 plane in the $n=3$ compound is significantly hole deficient.[30,31]

It is clear in Fig. 10(a) that, as in the case of the two-layer compound, the frequency of the $O(3)_{Bi}$ mode in (Bi,Pb)-2223 does not show a systematic variation with increasing oxygen concentration. Here we plot the Raman shift of this mode against hole concentration for $x=0.34$ (open circles), $x=0.40$ (open up triangles), and $x=0.60$ (open diamonds). The large experimental uncertainties might conceal any trends but possible changes in the position of this mode are evidently less than 6 cm^{-1}. As mentioned earlier, the impurity mode in the $n=3$ samples is significantly narrower than in the $n=2$ samples and hence it is possible to investigate the changes in the position of this peak with increasing oxygen or increasing Pb content. However, we show in Fig. 10(b) that, for both $x=0.34$ (open circles) and $x=0.40$ (open up triangles), there is no systematic change in the position of this peak with either oxygen or Pb content.

CONCLUSION

In conclusion, we find that the $O(2)_{Sr}$ mode Raman mode in ceramic samples of the $n=2$ and $n=3$ phases of the $Bi_{2.1-x}Pb_xSr_{1.9}Ca_{n-1}Cu_nO_{4+2n}$ superconductor systematically decreases with increasing hole concentration. This decrease is caused by additional oxygen in the weakly coupled BiO layers and any charge transfer effects are negligible. We also show that, contrary to previous reports by Kakihana *et al.*, charge transfer effects are negligible in $Bi_2Sr_2Ca_{1-z}Y_zCu_2O_{8+\delta}$ and that approximately one half of the measured shift in the frequency of the $O(2)_{Sr}$ mode can be attributed to oxygen compensation. We speculate that the correlation with increasing oxygen content arises from additional oxygen in the weakly coupled BiO layers leading to an expansion of the Cu-O-Bi bond length. We find that our data are consistent with the recent interpretation of the ~655 cm^{-1} mode in terms of a Cu-O-Bi vibration at the boundaries of the supercell. It is also clear that the ~540 cm^{-1} peak is due to an impurity phase rather than a Cu-O-Pb mode. The effect of Pb on the position of the Cu-O-Bi Raman mode, while being systematic, cannot yet be conclusively explained. We speculate that it may arise from a partitioning of Pb between the Bi, Sr, and Ca sites that changes with increasing Pb concentration and the additional holes introduced by Pb being compensated for by a decrease in oxygen content.

ACKNOWLEDGMENTS

We thank American Superconductor Corporation for their support and for tape samples. We acknowledge funding from the New Zealand FRST, The Royal Society of New Zealand, the United Kingdom EPSRC, and the Alexander von Humboldt Foundation.

[1] A. Bussmann-Holder, A. R. Bishop, L. Genzel, and A. Simon, Phys. Rev. B **55**, 11 751 (1997).
[2] A. Nazarenko and E. Dagotto, Phys. Rev. B **53**, 2987 (1996).
[3] M. Kakihana, M. Osada, M. Käll, L. Börjesson, H. Mazaki, H. Yasuoka, M. Yashima, and M. Yoshimura, Phys. Rev. B **53**, 11 796 (1996).
[4] J. Sapriel, J. Schneck, J. F. Scott, J. C. Tolédano, L. Pierre, J. Chavignon, C. Daguet, J. P. Chaminade, and H. Boyer, Phys. Rev. B **43**, 6259 (1991).
[5] R. G. Buckley, M. P. Staines, and H. J. Trodahl, Physica C **193**, 33 (1992).
[6] H. J. Trodahl, R. G. Buckley, and C. K. Subramaniam, Phys. Rev. B **47**, 11 354 (1993).
[7] X. H. Chen, K. Q. Ruan, G. G. Quin, S. Y. Li, L. Z. Cao, J. Zou, and C. Y. Xu, Phys. Rev. B **58**, 5868 (1998).
[8] J. L. Tallon, R. G. Buckley, M. R. Presland, P. W. Gilberd, I. W. M. Brown, M. Bowden, and R. Goguel, Phase Transit. **19**, 171 (1989).
[9] G. V. M. Williams, J. L. Tallon, R. Meinhold, and A. Janossy, Phys. Rev. B **51**, 16 503 (1995).
[10] A. E. Pantoja, D. M. Pooke, H. J. Trodahl, and J. C. Irwin, Phys. Rev. B **58**, 5219 (1998).
[11] R. Liu, M. V. Klein, P. D. Han, and D. A. Payne, Phys. Rev. B **45**, 7392 (1992).
[12] A. A. Tsvetkov, D. Dulić, D. van der Marel, A. Damascelli, G. A. Kaljushnaia, J. I. Gorina, N. N. Senturina, N. N. Kolesnikov, J. F. Ren, J. H. Wang, A. A. Menovsky, and T. T. M. Palstra, Phys. Rev. B **60**, 13 196 (1999).
[13] C. Kendziora, S. B. Qadri, and E. Skelton, Phys. Rev. B **56**, 14 717 (1997).
[14] M. Osada, M. Kakihana, M. Käll, L. Börjesson, A. Ioue, and M. Yashima, Phys. Rev. B **56**, 2847 (1997).
[15] Y. Stoto, D. Pooke, L. Forro, and K. Kishio, Phys. Rev. B **54**, 16 147 (1996).
[16] K. T. Wu, A. K. Fischer, V. A. Maroni, and M. W. Rupich, J. Mater. Res. **12**, 1195 (1997).
[17] M. R. Presland, J. L. Tallon, R. G. Buckley, R. S. Liu, and N. E. Flower, Physica C **176**, 95 (1991).
[18] S. D. Obertelli, J. R. Cooper, and J. L. Tallon, Phys. Rev. B **46**, 14 928 (1992).
[19] P. Krisnaraj, M. Lelovic, N. G. Eror, and U. Balachandran, Physica C **246**, 271 (1995).
[20] J. Shimoyama, J. Kase, T. Morimoto, J. Mizusaki, and H. J. Tagawa, Physica C **184-189**, 931 (1991).
[21] P. Ghigna, G. Spinolo, G. Flor, and N. Morgante, Phys. Rev. B **57**, 13 426 (1998).
[22] M. Osada, M. Kakihana, H. Arashi, M. Käll, and L. Börjesson, Phys. Rev. B **59**, 8447 (1999).
[23] R. D. Shannon, Acta Crystallogr., Sect. A: Cryst. Phys., Diffr., Theor. Gen. Crystallogr. **32**, 751 (1976).
[24] W. A. Groen, D. M. de Leeuw, and L. F. Feiner, Physica C **165**, 55 (1990).
[25] M. Cardona, R. Liu, C. Thomsen, M. Bauer, L. Genzel, W. König, A. Wittlin, U. Amador, M. Barahona, F. Fernandez, C. Otero, and R. Saez, Solid State Commun. **65**, 71 (1988).
[26] H. J. Rosen, R. M. Mcfarlane, E. M. Engler, V. Y. Lee, and R. D. Jacowitz, Phys. Rev. B **38**, 2460 (1988).
[27] N. Kijima, H. Endo, J. Tshuchiya, A. Sumiyama, M. Mizuno, and Y. Oguri, Jpn. J. Appl. Phys., Part 2 **28**, L787 (1989).
[28] A. Sequeira, J. V. Yakhmi, R. M. Iyer, H. Rajagopal, and P. V. P. S. S. Sastry, Physica C **167**, 291 (1990).
[29] W. A. Groen, D. M. de Leeuw, and G. M. Stollman, Solid State Commun. **72**, 697 (1989).
[30] R. Dupree, Z. P. Han, A. P. Howes, D. M. Paul, M. E. Smith, and S. Male, Physica C **175**, 269 (1991).
[31] A. Trokiner, L. Ne Noc, J. Schneck, A. M. Pougnet, R. Mellet, J. Primot, H. Savary, Y. M. Gao, and S. Aubry, Phys. Rev. B **44**, 2426 (1991).